Critical exponents of the two-layer Ising model

2001 J. Phys. A: Math. Gen. 34 6069

(http://iopscience.iop.org/0305-4470/34/31/302)

INSTITUTE OF PHYSICS PUBLISHING JOURNAL OF PHYSICS A: MATHEMATICAL AND GENERAL

J. Phys. A: Math. Gen. **34** (2001) 6069–6079 PII: S0305-4470(01)20260-1

Critical exponents of the two-layer Ising model

Z B Li[1,4], Z Shuai[2], Q Wang[3], H J Luo[3] and L Schülke[3]

[1] Zhongshan University, Guangzhou 510275, People's Republic of China
[2] Universitat de Mons-Hainaut, 7000 Mons, Belgium
[3] Universität Siegen, D-57068 Siegen, Germany

E-mail: LSchuelke@t-online.de

Received 21 December 2000, in final form 17 May 2001
Published 27 July 2001
Online at stacks.iop.org/JPhysA/34/6069

Abstract
The symmetric two-layer Ising model (TLIM) is studied by the corner transfer matrix renormalization group method. The critical points and critical exponents are calculated. It is found that the TLIM belongs to the same universality class as the Ising model. The shift exponent is calculated to be 1.773, which is consistent with the theoretical prediction of 1.75 with 1.3% deviation.

PACS numbers: 05.50.+q, 02.70.-c

(Some figures in this article are in colour only in the electronic version)

1. Introduction

The two-layer Ising model (TLIM), as a simple generalization of the two-dimensional Ising model and a simple model for the magnetic ultra-thin films, has been studied for a long time [1–6]. Cobalt films grown on a Cu(100) crystal, for instance, have highly anisotropic magnetization [7] and could therefore be viewed as layered Ising-spin systems. It has been found that capping PtCo in TbFeCo to form a two-layer structure has applicable features, for instance, raising the Curie temperature and reducing the switching fields for over-writable magneto-optical disks [8]. Apart from various possible applications to real physical materials, the model is theoretically interesting for its rich phase structure. The model has several interesting equivalents, such as a two-species gauge invariant Ising model [9], a spin-$\frac{3}{2}$ Ising model [10], a model of the dilute lattice gas and a quantum spin-$\frac{1}{2}$ ladder at zero temperature. The TLIM is important for the investigation of crossover from the two-dimensional Ising model to the three-dimensional one. In particular, it has been argued that the critical point of the latter could be found from the spectrum of the TLIM [11].

[4] Associate Member of ICTP, Trieste, Italy.

In recent years, some approximation methods have been applied to this model [10,12–18]. A critical line has been found in all these studies. As expected, the Curie temperature is very sensitive to the inter-layer interaction. Many discussions have been directed to the shift exponent at the decoupling point. Abe [3] and Suzuki [4] predicted $\gamma = 7/4$ for the isotropic model many years ago. Only in recent years have the computational results converged to the prediction, with still about 2.3% deviation [16, 17].

Apart from the shift exponent, it is also interesting to study the critical behaviour along the critical line. The model has the same critical exponents at the two ends of the critical line corresponding to the solvable decoupling limit and the infinite-interlayer-coupling limit, but it is clear that the decoupled system has a higher symmetry than the coupling layers, hence one cannot assume *a priori* that the TLIM belongs to the one-layer Ising universality class. Unusual finite-size effects have been observed in the dynamic process [19]. It has been proposed that the critical exponents (or some of them) would vary continuously along the critical line [9, 17]. However, there are also arguments in favour of unchanged exponents. Based on their correlation length equality method, Angelini *et al* [13] argued that the exponent ν is a constant. The accurate computation of critical exponents along the critical line remains a difficult unsolved problem.

It is our purpose to provide a reliable prediction for the critical exponents based on the corner transfer matrix renormalization group (CTMRG) method [20–22].

The CTMRG method follows White's idea of the density matrix renormalization group [23, 24]. It reduces the phase-space dimensions by omitting the eigenstates corresponding to small eigenvalues of the density matrix, but instead of constructing the density matrix through a series of column transfer matrices, Nishino and Okunishi made use of the corner transfer matrices. The CTMRG method has shown many merits for the two-dimensional classical models which can be mapped into interaction-around-face (IRF) models. Since the system can be easily extended to very large lattices, the finite-size effect can be ignored. The error mainly originates from the finite dimensions of the renormalized phase space, which only becomes severe for huge lattices at or very close to the critical point. Numerically it has been observed that the extrapolation from the finite-size scaling can provide very accurate information about the criticality.

We will focus on the TLIM composed of two identical layers. In this case, the model has a symmetry of interchanging the spins of the two layers. This symmetry is vital to the critical behaviour of the model. A breakdown of universality due to a small symmetry breaking [17] has been observed. In order to keep this symmetry, special care should be taken in the programming. Technically, the symmetry reduces the dimensions of the transfer matrix remarkably, but the extra degeneracy will slow down the convergence of the iteration, which makes the problem much more difficult compared to the one-layer Ising model.

The critical behaviour can be easily observed in various quantities, such as the rapid increase of the magnetization, the lambda peak of the capacity and the anomalous slowing down of convergence of the renormalization group iterations. However, to calculate the critical exponents, one needs to locate the critical points to high precision. This is done by a careful extrapolation of the renormalization dimension m.

In section 2, the TLIM is defined and transformed into an IRF model which is suitable for the CTMRG study. In the same section, the CTMRG method particular for the considered model will be introduced. The finite-size scaling and the finite-renormalization-dimension effect is studied in section 3. At the same time as the critical points are located, critical exponents of the scaling law are computed. Results for the critical exponents η and ν can also be found in section 3. Discussions and conclusions are given in the last section.

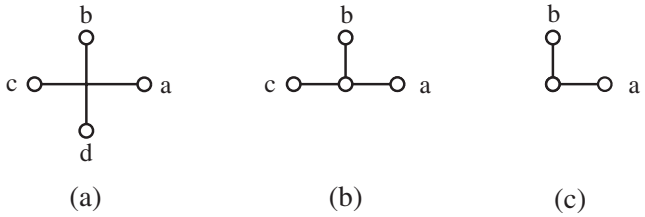

Figure 1. (*a*) A full vertex weight W_{abcd}; (*b*) an edge vertex weight W_{abc}; (*c*) a corner vertex weight W_{ab}.

2. The CTMRG method for the TLIM

The Hamiltonian of the model is defined by

$$H = -J_1 \sum_{\langle i,j\rangle} s_i s_j - J_2 \sum_{\langle i,j\rangle} \sigma_i \sigma_j - \lambda \sum_i s_i \sigma_i \tag{1}$$

where $s_i = \pm 1$ and $\sigma_i = \pm 1$ are Ising spins on two identical square lattices. For concreteness, let us say, s_i is at the site i of layer 1 and σ_i is at the corresponding site of layer 2, which is also labelled by i. Then $\langle i, j\rangle$ should be understood as a nearest-neighbour pair of sites on either layer 1 or 2, depending on which of the spin variables, s or σ, is concerned. In this paper, we only discuss the symmetric ferromagnetic case with nearest-neighbour coupling $J_1 = J_2 = J > 0$ and with interlayer coupling $\lambda = \rho J > 0$.

To obtain the equivalent IRF model, two species of Ising spins, $u_{ij} = \pm 1$ and $v_{ij} = \pm 1$, are introduced for each link $\langle i, j\rangle$. The Hamiltonian (1) is generalized to

$$H' = -J' \left[\sum_{\langle i,j\rangle} u_{ij}(s_i + s_j) + \sum_{\langle i,j\rangle} v_{ij}(\sigma_i + \sigma_j) + \rho' \sum_i s_i \sigma_i \right] \tag{2}$$

where J' and ρ' are defined as

$$J' = \tfrac{1}{2} \ln \left(\mathrm{e}^{2J} + \sqrt{\mathrm{e}^{4J} - 1} \right) \tag{3}$$

$$\rho' = \frac{\rho J}{J'}. \tag{4}$$

It is not difficult to show that, by summing over all u- and v-spins, the TLIM is recovered apart from a overall irrelevant constant factor to the partition function. Inversely, if the s- and σ-spins are summed, one will obtain the IRF model with four u-spin interactions and four v-spin interactions around each vertex. The vertex weight of the IRF model is given by

$$W_{abcd} = \sum_{s,\sigma=\pm 1} \exp\left\{ J' \left[s(u_a + u_b + u_c + u_d) + \sigma(v_a + v_b + v_c + v_d) + \rho' s\sigma \right] \right\} \tag{5}$$

where a, b, c and d denote the four (u, v)-spin pairs in the links joining to the vertex. Special weights in the boundary, which have links less than four, can be defined in a similar way as (5) but the values of s and σ are subject to the boundary condition. For instance, for the fixed boundary condition, the weight along the boundary, W_{abc}, is defined by

$$W_{abc} = \exp\left[J' \left(u_a + u_b + u_c + v_a + v_b + v_c + \rho' \right) \right]. \tag{6}$$

The vertex at the corner has a weight

$$W_{ab} = \exp\left[J' \left(u_a + u_b + v_a + v_b + \rho' \right) \right]. \tag{7}$$

They are schematically given in figures 1(*a*)–(*c*), respectively.

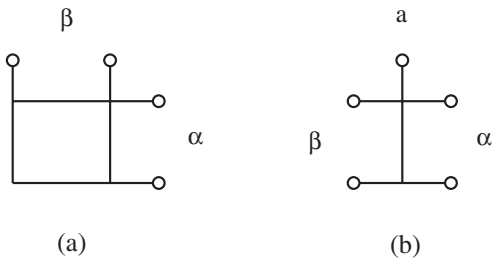

Figure 2. (*a*) A CTM, $C_{\alpha\beta}(2)$; a half-row transfer matrix (HRTM), $P_{\alpha\beta,a}(2)$.

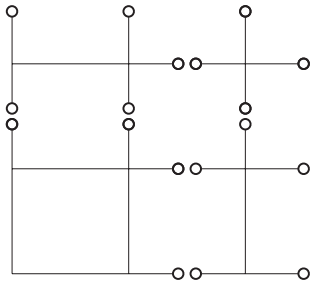

Figure 3. Enlarging $C_{\alpha\beta}(2)$ into $C_{\alpha\beta}(3)$.

The partition function is a trace of products of all vertex weights. The trace here means to sum over all spins. In the following, whenever two vertices are connected by a link, a summation over the (u, v)-spin pair in that link is implied. The vertex weights of a quarter lattice, after summation over all inner spins and boundary spins as it has been implied, is called a corner transfer matrix (CTM), denoted by $C_{\alpha\beta}(N)$. Here α and β denote the spin configurations of two open sides of the corner respectively, and N is the size of the corner. A schematic representation for a CTM is given in figure 2(*a*).

Another matrix we need is the so-called half-row transfer matrix (HRTM) denoted by $P_{\alpha\beta,a}(N)$. It is defined by the recursion relation

$$P_{\alpha\beta,a}(N) = \sum_{c} W_{abcd} P_{\alpha'\beta',c}(N-1) \tag{8}$$

$$P_{bc,a}(1) = W_{abc} \tag{9}$$

where α' and β' are spin configurations of two sides of the HRTM with size of $(N-1)$; c is the (u, v)-spin pair of the top of that HRTM and α and β are spin configurations of the enlarged HRTM with α representing (α', b) and β representing (β', d) respectively. For each value of a, $P_{\alpha\beta,a}(N)$ can also be considered as a matrix, denoted by $P_a(N)$. Figure 2(*b*) is an example of the HRTM.

In the process of the CTMRG iterations, the size of CTM is enlarged by one lattice spacing each time. This is done in the following way: (1) glue a HRTM to each open side of the CTM, (2) complement the bigger corner by adding a vertex weight. The recursion relation is

$$C_{\alpha\beta}(N) = \sum_{\alpha''\beta''} \sum_{cd} W_{abcd} P_{\alpha'\beta'',c}(N-1) \cdot C_{\alpha''\beta''}(N-1) P_{\alpha''\beta',d}(N-1). \tag{10}$$

It is schematically shown in figure 3.

By use of the CTM, the partition function of an even size lattice is simply the trace of the CTM to power four

$$Z_{2N} = \mathrm{Tr}(C(N)^4). \tag{11}$$

Therefore, the CTM and the density matrix have common eigenvectors. Denote the eigenvalues of C by $\{\omega_k | k = 0, 1, 2, \ldots\}$, assuming that $\omega_0 \geqslant \omega_1 \geqslant \omega_2 \geqslant \cdots$, the eigenvalues of the

density matrix are $\{\omega_k^4 | k = 0, 1, 2, \ldots\}$. According to the spirit of DMRG, only a certain number of the largest eigenstates will be kept. For instance, the first m eigenstates are kept; the eigenstates with smaller eigenvalues $\{\omega_k | k > m\}$ are ignored. m is the so-called renormalization dimension.

The CTMRG iterations contain the following steps: (i) construct $C(N)$ of a small CTM which is small enough to be exactly diagonalized; (ii) construct $P_a(N)$; (iii) diagonalize $C(N)$; (iv) if the dimension of $C(N)$ is smaller than m, all eigenstates are used as a basis of the renormalized phase space, otherwise only m eigenstates with the biggest eigenvalues are used as the basis; (v) by use of the eigenvectors which have been chosen for the renormalized space, form a projection operator $U(N)$ that projects old spin states into the renormalized space; (vi) use $U(N)$ to project $P_a(N)$ to the renormalized HRTM $P_a^r(N)$; (vii) form a diagonal matrix $C^r(N)$ by the first m largest eigenvalues, which is the renormalized CTM; (viii) use $P_a^r(N)$, $C^r(N)$ and the vertex weight W to form a bigger CTM, $C(N+1)$, and a bigger HRTM, $P(N+1)$, and repeat the above procedure from step (iii) with N replaced by $N+1$.

Since the renormalized phase space has dimension $\leqslant m$, the CTMRG in principle can go on infinitely. Therefore the lattice can be easily enlarged to very large sizes.

Particularly for the TLIM, it is efficient to choose the basis to be symmetric and antisymmetric in the exchange of two layers. In this way, the CTM is automatically block diagonal. The symmetric block and the antisymmetric block can be diagonalized separately. This is not just allowing larger m and high precision, but is also essential for keeping the presumed symmetry between two layers.

For small interlayer coupling, there are many approximate degenerate eigenstates due to the layer symmetry. If one does not separately consider the symmetric and antisymmetric phase space, it is easy to destroy the layer symmetry in the renormalization procedure.

Following the method of Nishino and Okunishi [20], the magnetization M can be calculated on an odd size lattice which is constructed by inserting an HRTM matrix between two adjacent CTM matrices and adding a proper vertex at the lattice centre. The probability that the central site has a spin state (s, σ) is given by

$$M^{s\sigma} = \frac{\sum_{abcd} X_{abcd}^{s\sigma} \operatorname{Tr}\left(P_a^r C^r P_b^r C^r P_c^r C^r P_d^r C^r\right)}{\sum_{abcd} W_{abcd} \operatorname{Tr}\left(P_a^r C^r P_b^r C^r P_c^r C^r P_d^r C^r\right)} \tag{12}$$

where $X_{abcd}^{s\sigma}$ is defined by

$$X_{abcd}^{s\sigma} = \exp\left\{J'\left[s(u_a + u_b + u_c + u_d) + \sigma(v_a + v_b + v_c + v_d) + \rho' s\sigma\right]\right\}. \tag{13}$$

The magnetization of layer 1, $M = \langle s \rangle$, is

$$M = M^{++} + M^{+-} - M^{--} - M^{-+}. \tag{14}$$

Due to the layer symmetry, it is also one-half of the total magnetization. The local energy density E can be calculated in a similar way.

$$E = \frac{\sum_{abcd} Y_{abcd} \operatorname{Tr}\left(P_a^r C^r P_b^r C^r P_c^r C^r P_d^r C^r\right)}{\sum_{abcd} W_{abcd} \operatorname{Tr}\left(P_a^r C^r P_b^r C^r P_c^r C^r P_d^r C^r\right)} \tag{15}$$

where

$$Y_{abcd} = \sum_{s,\sigma} X_{abcd}^{s\sigma} \ln(X_{abcd}^{s\sigma}). \tag{16}$$

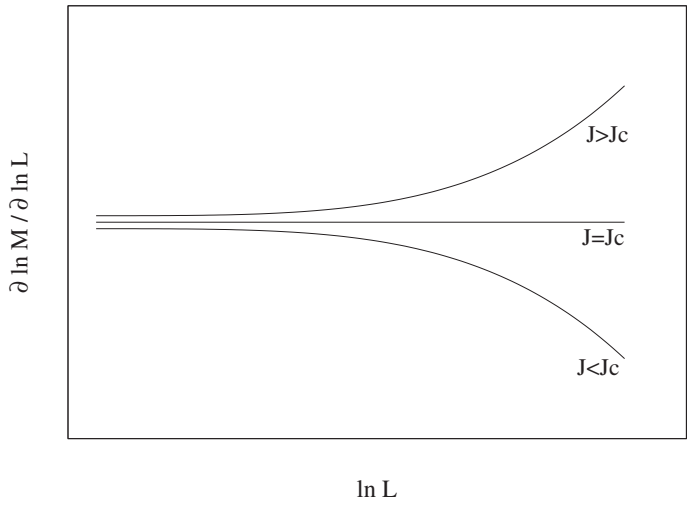

Figure 4. Schematic plot of the ideal curves $\partial \ln M/\partial \ln L$ versus $\ln L$.

3. Extrapolation and finite-size scaling

At the critical point J_c, it is expected that M obeys the finite-size scaling form $M \sim L^{-(d-2+\eta)/2}$, where L is the lattice size, so

$$\ln M(L) = \text{const} - \frac{d-2+\eta}{2} \ln L. \tag{17}$$

If we calculate $\partial \ln M/\partial \ln L$ and plot it with $\ln L$ as the horizontal axis, the curve should be a horizontal line for the critical point J_c with the vertical value of the line as $-(d-2+\eta)/2$. For J near J_c, there should be deviations from the power-law behaviour. A simple physics consideration reveals that the curves should be in the form shown in figure 4. So by searching for the 'best' horizontal line, one can determine the critical point J_c as well as the critical exponent η.

Things are not so easy, however. Figure 5 shows the curves of $\partial \ln M/\partial \ln L$ against $\ln L$ for $\rho = 0.1$, $J = 0.397\,726$ with different renormalization dimensions m. This J value is quite near to J_c. For small L, there exists a region where the lattice size is too small and finite-size scaling has not come into play. We will refer to this region as the small-size region. As L increases, the number of states of the system increases while the renormalization dimension m remains unchanged, and we will suffer from the 'finite-m effect' in due time. To obtain a more complete knowledge of the finite-m effect, let us look at figure 6, where curves for different J with $m = 60$ are shown. $m = 60$ is relatively small in our calculation and it has a more drastic finite-m effect. When L is small, all three curves shown in figure 6 increase, which is an indication of the small-size effect. After a certain value of L, one of the curves begins to bend down and the other two become much flatter. Here the critical behaviour dominates. However, the finite-m effect soon shows itself by raising the curves, which is also demonstrated clearly in figure 5. As a result, only approximately the part inside the dotted-line box resembles figure 4. It is hard to tell exactly where the finite-m effect begin to dominate without comparison with curves of higher m.

Nevertheless, some useful information can be drawn from the analysis. If a curve bends down for a period of L, one can judge that it corresponds to a J that is smaller than J_c. In other words, if a curve has a local maximum, it corresponds to a J with $J < J_c$. Thus the point

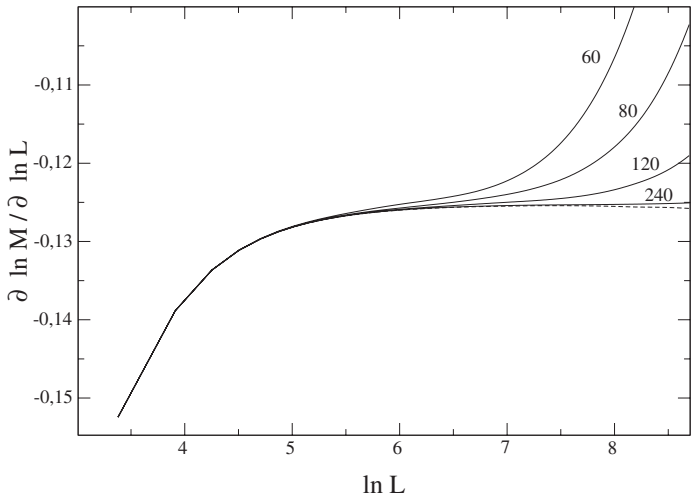

Figure 5. $\partial \ln M/\partial \ln L$ plotted versus $\ln L$ for $\rho = 0.1$, $J = 0.397\,726$. The solid curves are for $m = 60, 80, 120, 240$. The dashed curve is the result of an extrapolation to $m \to \infty$.

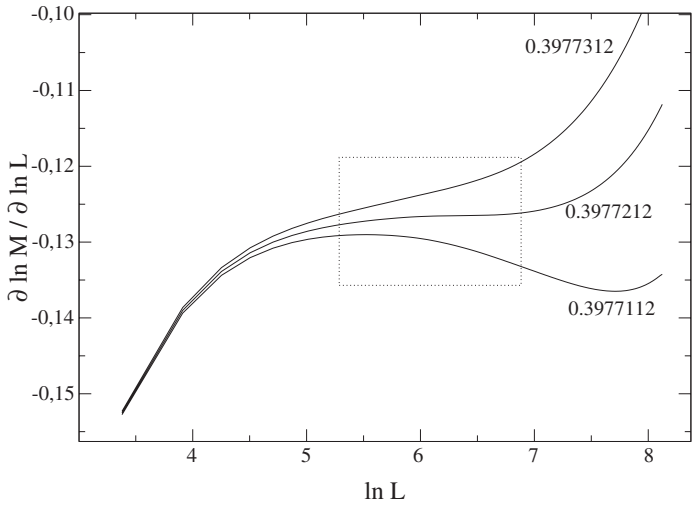

Figure 6. $\partial \ln M/\partial \ln L$ plotted versus $\ln L$ for $\rho = 0.1$, $m = 60$, for three different values of J.

now is to find $J_c^{(60)}$, above which the corresponding curve has no local maximum and below which it has. $J_c^{(60)}$ can be understood as a lower limit for J_c. In general, one can obtain $J_c^{(m)}$ as an estimate of J_c. The former will approach the latter from below as $m \to \infty$. Meanwhile the vertical value of the horizontal part of the curve with $J = J_c^{(m)}$ gives the estimate for $(d - 2 + \eta)/2$. To make the above discussion simpler, we have limited it only to the case with behaviour similar to that of $\rho = 0.1$. Later we will see in figure 7 that the small-size effect may show itself differently as ρ changes. However, similar analyses can still be developed for other cases.

In most of our calculations, we chose m to be 60, 80, 120 and 240. For each m, we calculated the magnetization with a set of J values and then determined the critical point using

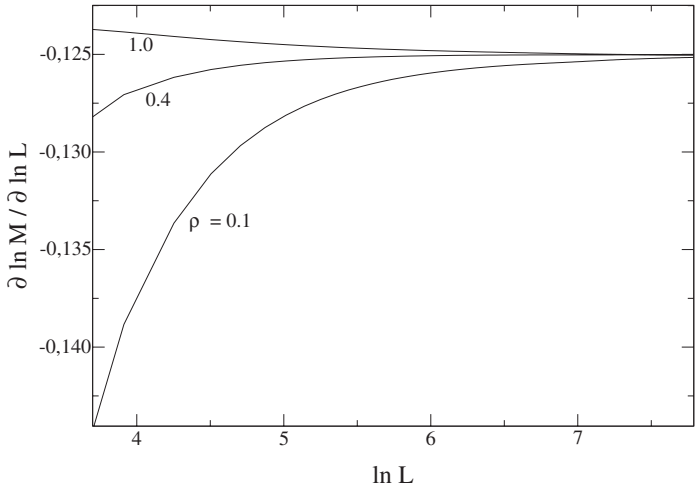

Figure 7. $\partial \ln M/\partial \ln L$ plotted versus $\ln L$ for $J = J_c$ with $\rho = 1.0, 0.4, 0.1$ from above, respectively.

Table 1. The critical point and critical exponent $(d-2+\eta)/2$ at $\rho = 0.1$ estimated through first looking for the flattest curve of $\partial \ln M/\partial \ln L \sim \ln L$ for a certain m then extrapolating to infinite m.

m	$J_c^{(m)}$	$(d-2+\eta)/2$
60	0.397 7212	0.126 29
80	0.397 7230	0.126 20
120	0.397 7252	0.125 48
240	0.397 7260	0.125 29
∞	0.397 7264	0.125 20

the method described above. The results for $\rho = 0.1$ are shown in table 1. The last row shows the extrapolated values for $m = \infty$.

An alternative and finer way for dealing with the finite-m problem is to extrapolate the data to $m \to \infty$ first and then analyse the extrapolated data. The extrapolation should lead to reasonable and smooth curves for $m = \infty$, and we assume the data converge monotonically as $m \to \infty$. This defines our criterion for choosing the extrapolation formula. We still take as an example the case with $J = 0.397\,726$, $\rho = 0.1$, whose curves are plotted in figure 5. For each value of lattice size L, we fit the points $(1/m, M^{(m)}(L))$, where $m = 60, 80, 120, 240$, with

$$y = a_5 x^5 + a_4 x^4 + a_3 x^3 + a_0. \tag{18}$$

a_0 then is considered to be the value for $m = \infty$ (see figure 8). Equation (18) does not include terms of x^1 and x^2 because including them violates the criteria above. The extrapolated curve is also shown in figure 5 as a dashed line.

Now that we have obtained the curves for $m = \infty$ with different J, we can search for the J value whose $\partial \ln M/\partial \ln L \sim \ln L$ curve is closest to a horizontal line. This J value is then the estimate of J_c. In our calculation, we use an interpolation technique to help locate the 'best' J, as shown in figure 9. The solid lines are those extrapolated to infinite m. We can obtain the magnetization for any value of J that is between $J = 0.397\,726$, for which the curve bends down, and $J = 0.397\,727$, where the line bends up, by linear interpolation. We found J_c to be 0.397 7262 with $(d-2+\eta)/2 = 0.125\,07$.

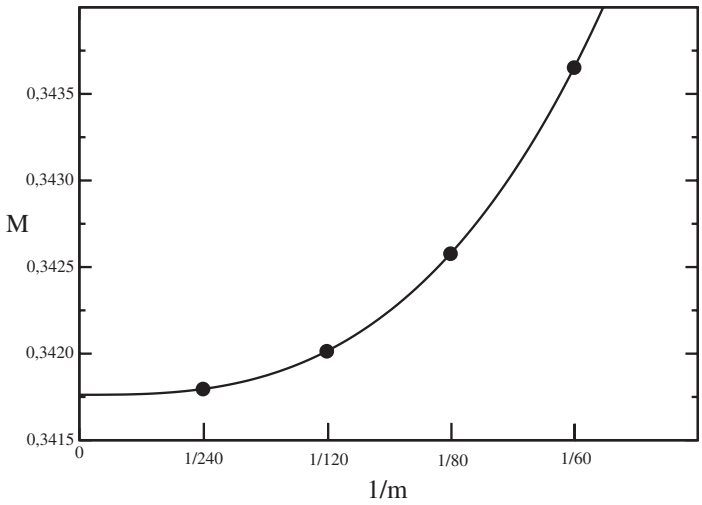

Figure 8. Extrapolation from $m = 60, 80, 120, 240$ for $J = 0.397\,726$, $\rho = 0.1$ and $L = 2001$.

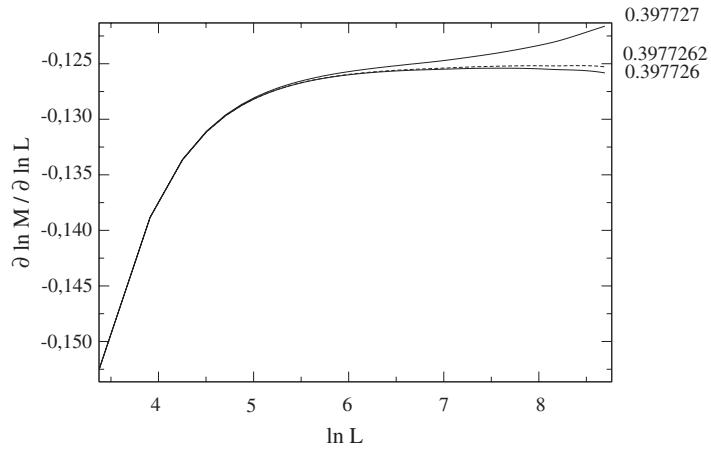

Figure 9. $\partial \ln M/\partial \ln L$ plotted versus $\ln L$ for $\rho = 0.1$. The solid lines are the extrapolated curves for $J = 0.397\,726$ and $J = 0.397\,727$. The dashed line is obtained from an interpolation between the two values of J.

The small-size effect for different ratios is presented in figure 7. For small ρ, this effect is big. In the case of $\rho = 0.1$, for instance, the small-size effect is visible with L up to 800. However, it seems that we overcome the small-size effect with $L = 2000$.

Having J_c in hand, we can determine another critical exponent ν through the finite-size scaling form of the energy density

$$E(L) - E_\infty \sim L^{-(d-\frac{1}{\nu})}. \tag{19}$$

The critical point J_c, critical exponents $(d - 2 + \eta)/2$ and $d - \frac{1}{\nu}$ for $\rho = 0.1, 0.4$ and 1.0 are collected in table 2.

For small ρ, the critical point $J_c(\rho)$ follows a power law $J_c(\rho) - J_c(0) \sim \rho^{1/\psi}$ with ψ the so-called shift exponent. With critical points for two small ρ in hand, the shift exponent

Table 2. Critical point J_c and critical exponents for $\rho = 0.1, 0.4$ and 1.0, estimated through first extrapolating the curve of $\partial \ln M/\partial \ln L \sim \ln L$ for infinite m then looking for the flattest curve.

ρ	$J_c^{(\infty)}$	$(d-2+\eta)/2$	$d-\frac{1}{\nu}$
0.1	0.397 7262	0.125 07	1.0014
0.4	0.354 1412	0.125 03	1.0001
1.0	0.311 7577	0.125 02	0.9996

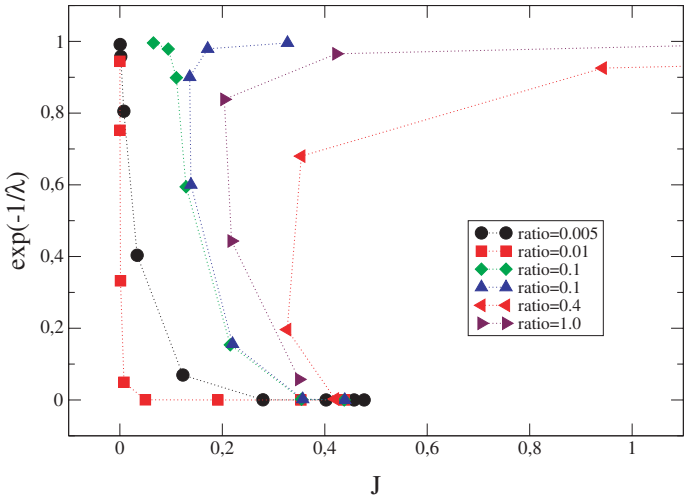

Figure 10. The RG trajectories mapped to the TLIM parameter space are plotted. The vertical axis is $\exp(-1/\lambda)$ with $\lambda = \rho J$. Corresponding to the curves in the order of the legend, the starting couplings are $J = 0.477, 0.438, 0.438, 0.439, 0.42$ and 0.35, respectively.

can be estimated by

$$\psi = \ln\left(\frac{\rho_1}{\rho_2}\right) \Big/ \ln\left(\frac{J_c(\rho_1) - J_c(0)}{J_c(\rho_2) - J_c(0)}\right) \tag{20}$$

where $J_c(0)$ is known as the critical point of the one-layer Ising model. For $\rho = 0.005$ and 0.01, we find the critical points $J_c = 0.432\,507$ and $0.428\,593$, respectively, which lead to $\psi = 1.773$, consistent with the theoretical prediction $\psi = \gamma = 1.75$ within 1.3% deviation.

4. Discussion and conclusions

Our numerical results suggest that the TLIM model is in the Ising universality class. That is, for a finite interlayer coupling, the critical behaviour of the TLIM is the same as that of the one-layer system. Both $\langle s \rangle$ and $\langle \sigma \rangle$ are order parameters in the transition. Our observations strongly exclude a phase transition for the electric order, except at the decoupling point $\rho = 0$.

The critical line of the TLIM is in fact not a fixed line since the interlayer coupling is a relevant interaction, which should flow to infinity in renormalization group transformations. Then the TLIM resembles the one-layer Ising model in the long-range critical behaviour. To confirm this picture, we also carry out the real-space renormalizational group transformation to the model. The lattice is divided into 3×3 blocks. All nearest-neighbour interactions are kept. The RG trajectories are plotted in figure 10. Two attractive fixed points both having infinite ρ

are observed. They are the ordered and disordered fixed points, respectively. Figure 10 shows that the renormalization trajectories always flow to infinite ρ except for that starting at $\rho = 0$, which remains zero and corresponds to the one-layer Ising fixed point $J_c(0)$. The trajectory which flows from $J_c(0)$ to $J_c(\infty) = J_c/2$ and which separates two attractive points should be the critical line obtained in the present and previous papers. Therefore we conclude that there is no fixed line for finite ρ.

However, as the interlayer coupling is small, it needs a large scale transformation to reach the infinite fixed points, so the model has extraordinarily large finite-size effects, as we have observed in the numerical results.

The decoupling limit shows singularities due to the existence of the severe competition between the unstable decoupling fixed point and the attractive infinite interlayer coupling fixed points, which, however, are far away. This is supported in some sense by the unusual sensitivity of the shift exponent to the couplings [16, 17] and the strange layer symmetry breaking in the effective state at the decoupling limit [14]. Our estimate for the shift exponent is consistent with the theoretical prediction.

The unusual small-size effects will have important consequences for the local properties of the TLIM. These are manifested in the short-time critical behaviour that we recently observed in Monte Carlo simulations, which will be reported elsewhere [19].

Acknowledgments

The authors thank B Zheng for helpful discussions. This work was supported by the National Natural Science Foundation of China under project 19772074 and by the Deutsche Forschungsgemeinschaft under project Schu 95/9-3.

References

[1] Ballentine L E 1964 *Physica* **30** 1231
[2] Allan G A T 1970 *Phys. Rev.* B **1** 352
[3] Abe R 1970 *Prog. Theor. Phys.* **44** 339
[4] Suzuki M 1971 *Prog. Theor. Phys.* **46** 1054
[5] Binder K 1974 *Thin Solid Films* **20** 367
[6] Oitmaa J and Enting G 1975 *J. Phys. A: Math. Gen.* **8** 1097
[7] Oepen H E, Benning M, Ibach H, Schneider C M and Kirschner J 1990 *J. Magn. Magn. Mater.* **86** L137
[8] Shimazaki K, Ohnuki S, Fujiwara H and Ohta N 1992 *J. Magn. Magn. Mater.* **104–107** 1017
[9] Li Z B, Schülke L and Zheng B 1994 *Preprint* University of Siegen
[10] Horiguchi T, Lipowski A and Tsushima N 1996 *Physica* A **224** 626
[11] Wosiek J 1994 *Phys. Rev.* B **49** 15023
[12] Angelini L, Caroppo D, Pellicoro M and Villani M 1992 *J. Phys. A: Math. Gen.* **25** 5423
[13] Angelini L, Caroppo D, Pellicoro M and Villani M 1995 *Physica* A **219** 447
[14] Angelini L, Caroppo D, Pellicoro M and Villani M 1997 *Physica* A **237** 320
[15] Lipowski A and Suzuki M 1993 *Physica* A **198** 227
[16] Lipowski A and Suzuki M 1998 *Physica* A **250** 373
[17] Horiguchi T and Tsushima N 1997 *Physica* A **238** 295
[18] Hu C, Izmailian N S and Oganesyan K B 1999 *Preprint* cond-mat/9904008
[19] Li Z B, Luo H J, Schülke L and Wang Q *Preprint*
[20] Nishino T and Okunishi K 1996 *J. Phys. Soc. Japan* **65** 891
[21] Nishino T, Okunishi K and Kikuchi M 1996 *Phys. Lett.* A **213** 69
[22] Nishino T and Okunishi K 1997 *J. Phys. Soc. Japan* **66** 3040
[23] White S R 1992 *Phys. Rev. Lett.* **69** 2863
[24] White S R 1993 *Phys. Rev.* B **48** 10345